ELSEVIER

International Journal of Mass Spectrometry 182/183 (1999) 45–52

International Journal of Mass Spectrometry

Hypermetallic dilithium fluoride, Li_2F, and its cation and anion: a combined dissociation and charge permutation study

Michael J. Polce, Chrys Wesdemiotis*

Department of Chemistry, The University of Akron, Akron, OH 44325, USA

Received 17 July 1998; accepted 10 September 1998

Abstract

Dilithium fluoride, Li–F–Li, has been produced in the gas phase by neutralization of the Li_2F^+ cation, generated by fast atom bombardment ionization of lithium trifluoroacetate. Subsequent reionization after ~0.2 μs conclusively shows that the hypermetallic fluoride Li_2F has survived intact and, thus, exists as a bound species. Charge reversal of Li_2F^+ reveals that the anion Li_2F^- is stable also. These results are in agreement with previous results of ab initio calculations which predict considerable binding energies (≥129 kJ mol^{-1}) for radical Li_2F and anion Li_2F^-, both of which violate the octet rule. Collisionally excited Li_2F^+ cations dissociate to Li^+, $LiF^{+\cdot}$, $Li_2^{+\cdot}$, and F^+ fragments. The yield of F^+ strongly depends on the collision gas used, maximizing with He and Ne targets whose ionization energies lie above that of the fluorine atom. (Int J Mass Spectrom 182/183 (1999) 45–52) © 1999 Elsevier Science B.V.

Keywords: Dilithium fluoride; Hypermetalated or hypermetallic species; Superalkalis; Neutralization-reionization

1. Introduction

Dilithium fluoride, Li_2F, belongs to the class of hypermetalated or hypermetallic molecules. This term describes species containing two or more metal atoms in stoichiometries that exceed normal valence expectations [1–4]. Other examples are OLi_4 [1], CLi_6 [2], $HONa_2$ [4], $HSNa_2$, Al_3O [5], and Mg_2O [6]. For all these species, which resemble metal clusters bound to a central more electronegative moiety, theory predicts substantial thermodynamic stability due to the presence of bonding between the metal and central atoms as well as metal–metal bonding [1–6]. A special family of hypermetalated compounds are the superalkalis, $M_{k+n}X$, where M is an alkali metal atom, X the central moiety, k the normal valency of the central moiety and $n \geq 1$ [1–9]. Such molecules are considered to be superalkaline because of their extremely low ionization energy (IE), which commonly lies below that of the corresponding alkali metal; e.g. IE(Na) = 5.14 eV versus IE(Na_3O) = 3.90 eV [10].

Hypermetalated species are possible intermediates in metal cluster and metal surface reactions which can affect the catalytic and electronic properties of a metal; they also reveal fundamental information about the relationship between hypervalency and stability. As a result, the structures and bonding characteristics of hypermetalated molecules have been studied extensively by theory [1–9,11]. Experimental investiga-

* Corresponding author.

Dedicated to the memory of Professor Ben S. Freiser for his numerous and significant contributions to gas phase organometallic chemistry.

PII S1387-3806(98)14234-3

tions have so far confirmed the existence of several superalkali compounds, including oxides ($M_{2+k}O$) [12–17], hydroxides ($K_{2-3}OH$) [18,19], sulfides ($Li_{3-4}S$) [20], phosphides (Li_4P) [21], halides (Na_2F [16], Na_2Cl [14]) [22], and cyanides (Li_2CN [23], K_2CN [24]), which were formed using Knudsen effusion cells [12,20,21,23], coexpanding or crossed molecular beams [13–17,22], flow reactors [18,19] or laser ablation [24]. These studies produced ionization energies and a few unresolved electronic band spectra. Here, we present the first application of neutralization–reionization mass spectrometry (NRMS) [25–30] to hypermetallic species. This tandem mass spectrometry technique is employed to probe the gas phase chemistry of the superalkali fluoride Li_2F, whose existence has been predicted by numerous computational studies [7–9].

With NRMS, a reactive neutral can be synthesized in the gaseous state by neutralization of the corresponding cation or anion, provided one of them is stable and independently available. The known Li_2F^+ ion [31–38] is used in this study as precursor for the elusive Li_2F. The stability and unimolecular reactivity of the neutral Li_2F radical generated this way are subsequently determined from the mass spectra arising after reionization to positive ions. In addition, charge reversal of Li_2F^+ [39] is used to obtain the first experimental evidence for the stability of anionic dilithium fluoride, Li_2F^-, which has recently been calculated to be a bound species [40,41]. Finally, the unimolecular chemistry of cationic Li_2F^+, which has not been characterized before, also is assessed.

2. Experimental

The experiments were performed with a modified Micromass AutoSpec E_1BE_2 tandem mass spectrometer (E, electrostatic analyzer; B, magnetic sector) that has been described in detail elsewhere [42]. The instrument is equipped with two collision cells (C-1 and C-2) and an intermediate ion deflector in the field-free region between E_1B (MS-1) and E_2 (MS-2). This configuration permits the acquisition of various types of tandem mass spectra (MS/MS) [43], including those resulting from collisionally activated dissociation (CAD) [43], neutralization–reionization (NR) [25–30] and charge reversal (CR) [39].

Li_2F^+ was formed by fast atom bombardment (FAB) of a saturated solution of lithium trifluoroacetate in glycerol. A few microliters of this solution was placed onto the stainless steel probe tip and bombarded with 20 keV Cs^+ ions. The ions desorbed during this process were accelerated to 8 keV before entering the E_1BE_2 mass analyzing section.

The MS/MS experiments on dilithium fluoride employed the $^7Li_2F^+$ isotopomer. CAD spectra were measured by mass-selecting Li_2F^+ through MS-1, subjecting it to high-energy (8 keV) collisions with various gaseous targets in C-2 (O_2, He, Ne, Ar, Xe) and separating the ionic fragments generated in this process by MS-2. For NR mass spectra, mass-selected Li_2F^+ was neutralized by collision with trimethylamine (TMA) in C-1; after concomitantly formed fragment ions and unreacted precursor ions were removed by deflection from the beam path, the remaining beam of neutral Li_2F was reionized to cations by collision with O_2 or He in C-2. The ions formed in the reionization step were mass-analyzed by MS-2 to yield the respective $^+NR^+TMA/Y$ spectrum, where the superscripts denote the charges of precursor and final product ions and Y the target used for reionization. Finally, $^+CR^-$ of Li_2F^+ was performed by collision of this cation with gaseous TMA in C-2 and mass analysis of the anions arising upon this process through MS-2. In all these experiments, the pressure of each collision gas was adjusted to effect approximately 20%–30% attenuation of the mass-selected main beam.

Kinetic energy releases were measured from peak widths at half height ($T_{0.5}$) and are corrected for the main beam width [44,45]. All spectra shown are multiscan summations and their relative abundances are reproducible within $\pm 15\%$. Lithium trifluoroacetate and glycerol were purchased from Aldrich and Fisher Scientific, respectively, and the collision gases were purchased from Linde (Ar, O_2), Liquid Carbonic (He), Matheson (TMA), or Praxair (Ne, Xe). All chemicals were used as received.

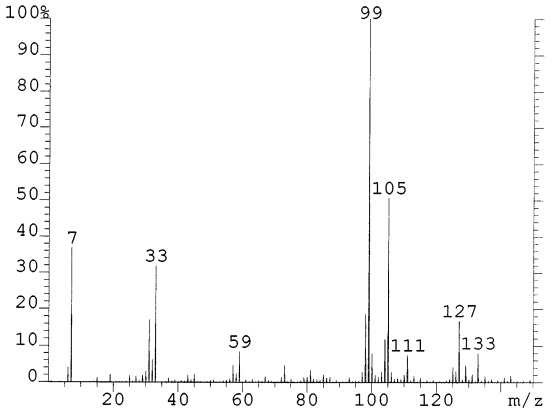

Fig. 1. FAB mass spectrum of lithium trifluoroacetate ($CF_3COO^-Li^+$) in glycerol matrix.

3. Results and discussion

3.1. Dilithium fluoride cation, Li_2F^+

Figure 1 displays a partial magnetic scan of the products formed upon FAB ionization of lithium trifluoroacetate; the major ^7Li containing ions are Li^+ (*m*/*z* 7), Li_2F^+ (33), $Li_3F_2^+$ (59), $[glycerol + Li]^+$ (99), $[glycerol–H + 2Li]^+$ (105), $[glycerol–2H + 3Li]^+$ (111) and $[CF_3CO_2Li + Li]^+$ (127).

Mass-selected Li_2F^+ cations undergo no detectable spontaneous dissociation. After collisional activation, however, they yield all four possible products, viz. Li^+ (*m*/*z* 7), $Li_2^{+\cdot}$ (14), F^+ (19), and $LiF^{+\cdot}$ (26), as documented by the CAD spectra of Fig. 2, for which O_2, He, Ne, Ar, and Xe were the collision gases. Important energy data concerning these fragmentations are summarized in Table 1 [10,41,46,47]. The dissociation energy of Li_2F^+ to Li^+, which is equivalent to the lithium ion affinity of LiF, is found computationally in the range 213–279 kJ mol^{-1} [8,32,33,37,40,41]; the value of 264 kJ mol^{-1} given in Table 1 stems from the most recent, highest level ab initio study by Gutowski and Simons [41]. No theoretical data are available about the critical energies of the other collision-induced fragmentations (leading to $Li_2^{+\cdot}$, F^+, and $LiF^{+\cdot}$), but based on the heats of formation of the corresponding reaction products (Table 1), these fragments must arise through higher energy processes.

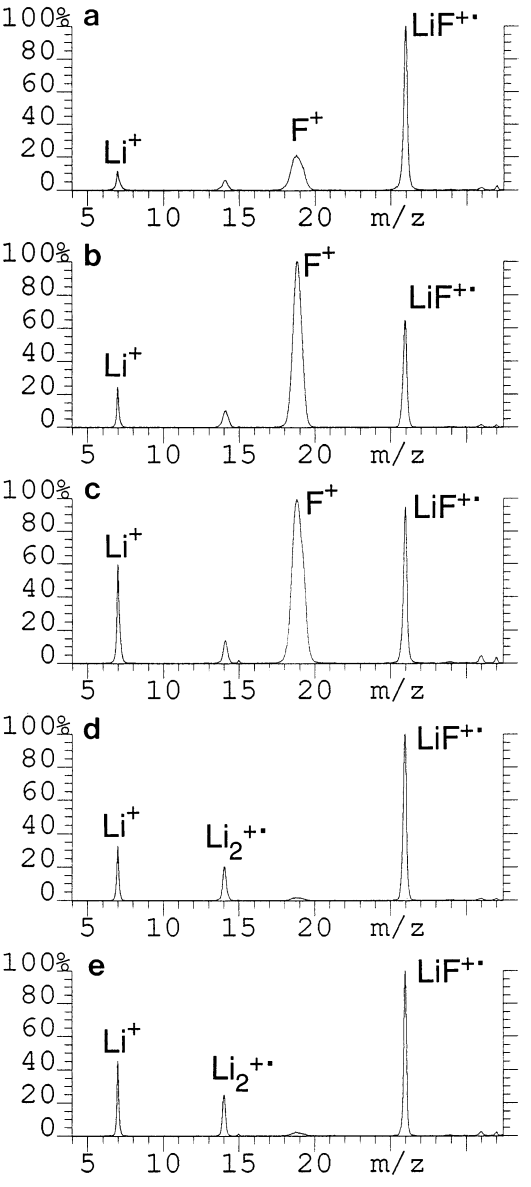

Fig. 2. CAD spectra of cation Li_2F^+ using different collision gases; (a) O_2, (b) He, (c) Ne, (d) Ar, and (e) Xe. The small peaks at *m*/*z* 32, 31, 29 and 15 are due to contamination by the isobaric $CH_3OH_2^+$ ion (from the FAB matrix).

We find the relative abundance of F^+ (*m*/*z* 19) to be strongly dependent on the CAD target (Fig. 2). With the gases used, $[F^+]$ follows the order He ≈

Table 1
Thermochemical data for the unimolecular reactions of Li_2F^+ and Li_2F (in kJ mol^{-1})[a]

Reaction	$\Sigma\Delta H_f^\circ$ (products)	D[b]
$Li_2F^+ \rightarrow Li^+$ (m/z 7) + LiF	350[c]	264[d]
$Li_2^{+\cdot}$ (m/z 14) + F	788	
Li_2 + F^+ (m/z 19)	1983	
Li + $LiF^{+\cdot}$(m/z 26)	871[e]	
$Li_2F \rightarrow$ Li + LiF	−177[c]	141[f]
Li_2 + F	295	

[a] From [10] if not noted otherwise.
[b] Calculated dissociation energy including zero-point vibrational energy (highest level values available).
[c] Using ΔH_f° (LiF) = −336 kJ mol^{-1} from [47].
[d] From [41].
[e] Using ΔH_f° ($LiF^{+\cdot}$) = 712 kJ mol^{-1} based on IE(LiF) = 10.86 eV, a computational value from [46].
[f] From [9].

Ne > O_2 ≫ Ar ≈ Xe. Moreover, the F^+ peak is markedly wider than those of the other fragments, indicating that F^+ formation proceeds with substantial release of internal into translational energy. For example, the kinetic energy releases ($T_{0.5}$) for Li^+, $Li_2^{+\cdot}$, F^+, and $LiF^{+\cdot}$ upon CAD/He are 0.06, 0.25, 0.73, and 0.14 eV, respectively; similarly, a sequentially acquired CAD/O_2 spectrum leads to $T_{0.5}$ = 0.07, 0.15, 1.20, and 0.12 eV. Although the absolute $T_{0.5}$ values depend on the collision gas and experimental conditions, they consistently increase in the order $T_{0.5}$ (Li^+, $LiF^{+\cdot}$) < $T_{0.5}$ ($Li_2^{+\cdot}$) < $T_{0.5}$ (F^+) in all CAD experiments.

There is consensus in the computational studies that ground-state Li_2F^+ has a linear Li^+–F^-–Li^+ structure ($D_{\infty h}$ geometry) with essentially ionic bonds [8,37,41]. Direct cleavages from this structure can account for the Li^+ and $LiF^{+\cdot}$ products. Since the potential energy minimum of Li^+–F^-–Li^+ is rather flat with respect to bending [33,36], rearrangements (such as $Li_2^{+\cdot}$ formation or Li_2 loss) are also feasible. Note that the rearrangements ($Li_2^{+\cdot}$, F^+) are found to yield broader peaks than the direct cleavages (Li^+, $LiF^{+\cdot}$), pointing out that the former may proceed with appreciable reverse activation energies; such reverse barriers are generally released into kinetic energy ($T_{0.5}$) upon dissociation (at least in part), thereby enhancing peak broadening [44,45]. Considering the high ionization energy of fluorine (17.4 eV [10]) and the charge distribution in Li^+–F^-–Li^+, the production of F^+, particularly in the extent observed with He and Ne targets, is surprising. Possibly, F^+ is formed from an excited electronic state of Li_2F^+, lying well above the energy level of the F^+ + Li_2 products; such a scenario would also explain the substantially larger kinetic energy release observed for F^+ versus the alternative rearrangement product $Li_2^{+\cdot}$. Finally, the yield of F^+ upon CAD appears to correlate with the ionization energy of the target. With the atomic targets used, viz. He (IE = 24.6 eV), Ne (21.6 eV), Ar (15.8 eV), and Xe (12.1 eV) [10], the F^+ intensity drops dramatically if the ionization energy of the target falls below that of fluorine, presumably because F^+ is largely neutralized by the target. With a molecular target, such as O_2 (IE = 12.1 eV), this charge exchange would be subject to Franck–Condon effects and would also depend on the orientation of the collision partners [25–30], justifying the higher abundance of F^+ upon CAD/O_2 versus CAD/Xe despite the very similar ionization energies of O_2 and Xe.

3.2. Neutral dilithium fluoride, Li_2F

Gas phase neutralization of Li_2F^+ (m/z 33) by TMA generates the incipient dilithium fluoride radical, which upon subsequent reionization with O_2 or He gives rise to the $^+NR^+$ mass spectra of Fig. 3. Both spectra contain significant Li_2F^+ recovery peaks (m/z 33), providing strong evidence that Li_2F has survived intact for the time window between the neutralization and reionization events (~0.2 μs). This

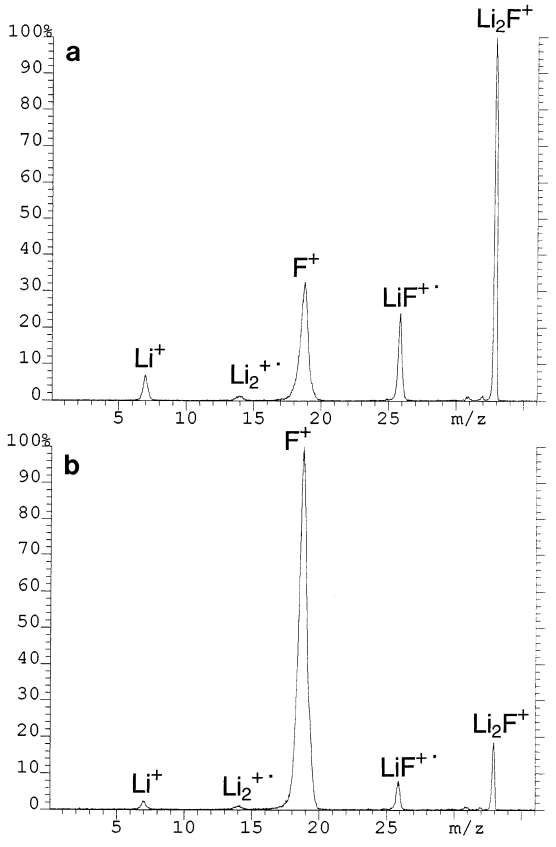

Fig. 3. (a) $^{+}NR^{+}$ TMA/O_2 and (b) $^{+}NR^{+}$ TMA/He spectra of Li_2F^+. For the tiny peaks at *m*/*z* 32 and 33 see the legend of Fig. 2 and the text.

result confirms numerous theoretical predictions that the superalkali Li_2F is a bound species, separated by 138 [8], 141 [9], or 129 kJ mol^{-1} [41] from the lowest energy dissociation products Li + LiF (Table 1); alternative dissociation channels, such as the formation of Li_2 + F, would have to overcome even higher barriers (Table 1).

Helium, which is known to deposit a higher average internal energy upon reionization than oxygen [48], expectedly causes more extensive fragmentation upon $^{+}NR^{+}$. With both targets, the most intense fragments are $LiF^{+\cdot}$(*m*/*z* 26) and F^+ (*m*/*z* 19), as is the case in the corresponding CAD spectra, too. Further, the kinetic energy releases upon fragmentation increase in the order $T_{0.5}$ (Li^+, $LiF^{+\cdot}$) < $T_{0.5}$ ($Li_2^{+\cdot}$) < $T_{0.5}$(F^+), in agreement with the trend observed upon CAD. These analogies suggest that the majority of the $^{+}NR^{+}$ fragment ions arise from neutralized–reionized Li_2F^+, not from the intermediate Li_2F radical. The $^{+}NR^{+}$ process is known to deposit higher average internal energies than CAD [49,50], which can adequately explain the differences in relative fragment ion abundances between $^{+}NR^{+}$ and CAD spectra.

Ab initio theory predicts a bent C_{2v} geometry for the global minimum of Li_2F ($^2A_1$ state) [7–9,41]. In this structure, the Li–F bonds are 1.68 Å long and the Li–F–Li angle has a value of 107.1° [8]. The calculated distance between the two lithium atoms (2.70 Å) lies very close to the bond length of Li_2 (2.78 Å) [8], indicating the occurrence of covalent Li–Li bonding in Li_2F. The calculated charges on the Li and F atoms of Li_2F are +0.50 and −1.00, respectively [8], thus allowing for attractive interactions between the central F atom and the Li ligands. The synergistic effect of electrostatic bonding between central atom and ligands and of covalent bonding between the ligands has been assumed by theory to be the origin of the high thermodynamic stability of hypermetalated radicals, such as Li_2F, which violate the octet rule by having more than eight valence electrons. This computationally indicated stability is corroborated by the discussed $^{+}NR^{+}$ data.

The barrier for linearization of the bent Li_2F radical (C_{2v}) is calculated to be quite small, viz. 11 [8] or 22 kJ mol^{-1} [41]; for comparison, the dissociation threshold to Li + LiF requires 129–141 kJ mol^{-1} (as mentioned previously). Thus, the Li–F–Li bond angle in the radical is quite flexible [7]. Further, the equilibrium bond lengths in Li_2F^+ and Li_2F are essentially identical (both 1.68 Å [8]). As a result, the vertical reduction of linear Li_2F^+ ($D_{\infty h}$) should yield ground-state Li_2F with little (if any) vibrational excitation and a favorable Franck–Condon factor [51]. The high abundance of the recovery peak (*m*/*z* 33) in the $^{+}NR^{+}$ spectra and the absence of any appreciable fragmentation of Li_2F in the time available between its formation and reionization (vide supra) validate this expectation.

Compared to the ionization energy of Li (5.39 eV [10]), that of Li_2F is theoretically predicted to be

significantly lower; specifically, adiabatic IE values of 3.87 and 3.93 eV have been calculated by Rehm et al. [8] and Gutowski and Simons [41], respectively. These values are fairly close to the vertical recombination energy of Li_2F^+, calculated by Gutsev and Boldyrev (3.64 eV) [7]. The predicted IEs disagree with a recent experimental estimate of 5.42 eV, derived by Veljković et al. [52] from the temperature dependence of the intensities of Li_2F^+ and Li^+ formed by surface ionization at a hot rhenium surface. The latter method assumes that desorbed Li_2F is the sole source of Li_2F^+; however, formation of Li_2F^+ via an ion–molecule reaction cannot be excluded and may cause the discrepancy between theoretical and experimental results. Irrespective of the exact adiabatic IE (Li_2F) value, neutralization of Li_2F^+ by TMA is endothermic by ~4.8 eV, which is the difference between the vertical ionization energy of TMA (8.4 eV [10]) and the vertical recombination energy of Li_2F^+ (3.64 eV [7]). The charge exchange reaction $Li_2F^+ + TMA \rightarrow Li_2F + TMA^{+\cdot}$ is still observed because the energy deficit can be supplied by the kinetic energy of Li_2F^+ (8 keV). Such strongly endothermic reactions often suffer from poor cross sections as compared to nearly thermoneutral neutralizations. Indeed, our total $^+NR^+$ yields (total ion flux in $^+NR^+$ spectra divided by flux of mass-selected precursor ion) are rather low, lying about 4×10^{-4} (for TMA/O_2 and TMA/He); for comparison, $^+NR^+$ TMA/O_2 of $C_2H_3N^+$ cations, where the neutralization process is close to thermoneutral, proceeds with a three times larger yield under similar experimental conditions [53].

Finally, it is noticed that the CAD and $^+NR^{+\cdot}$ spectra of Li_2F^+ (*m*/*z* 33) contain minor peaks at *m*/*z* 32, 31, 29, and 15. These ions cannot arise from Li_2F^+ and originate from an isobaric impurity from the glycerol matrix. FAB of pure matrix gives rise to a tiny *m*/*z* 33 ion whose CAD spectrum identifies it as the $CH_3OH_2^+$ cation. This contaminant does not affect the tandem mass spectra of Li_2F^+; neither does it contribute to the abundant Li_2F^+ recovery peak (*m*/*z* 33) in the $^+NR^+$ spectra of Fig. 3, because neutral CH_3OH_2 is unstable [54].

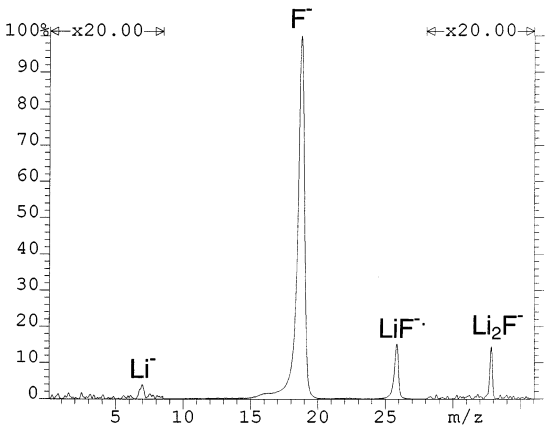

Fig. 4. $^+CR^-$ spectrum of Li_2F^+ with TMA targets.

3.3. Anionic dilithium fluoride, Li_2F^-

Charge reversal of Li_2F^+ with TMA targets gives rise to the $^+CR^-$ spectrum of Fig. 4. This spectrum contains a detectable Li_2F^- signal at *m*/*z* 33, showing that the dilithium fluoride anion is a stable species, capable of surviving intact for several microseconds (time needed by Li_2F^- to reach the detector). This result is consistent with ab initio theoretical studies [40,41], based on which Li_2F^- is bound by 69 kJ mol^{-1} (0.72 eV) with respect to electron detachment and by 140 kJ mol^{-1} with respect to dissociation into Li^- + LiF [41]. The $^+CR^-$ spectrum also includes logical fragments at *m*/*z* 26 ($LiF^{-\cdot}$), 19 (F^-) and 7 (trace, Li^-). The tail observed at the low-mass side of F^- is assigned to fluoride anions formed inside MS-2 (electrostatic analyzer), via metastable decay of Li_2F^- (or $LiF^{-\cdot}$). Interestingly, the relative abundances of the anions generated upon $^+CR^-$ are found to rise with the electron affinities of the corresponding neutrals, which are (in electron volts) 0.62 for Li, 0.72 for Li_2F, >1.35 for LiF and 3.40 for F [10,41].

Charge reversal of multiatomic cations to anions primarily takes place via stepwise addition of electrons [53,55]; hence, the dilithium fluoride anions emerging from the $^+CR^-$ process are most likely formed through the sequence $Li_2F^+ \rightarrow Li_2F \rightarrow Li_2F^-$. The ground electronic state of Li_2F^- is computationally found to have a linear $[Li–F–Li]^-$ structure ($D_{\infty h}$) with a geometry close to that of Li_2F^+ [41].

On the other hand, the ground state of the Li_2F radical has a bent C_{2v} geometry, as mentioned above. The vertical transition $Li_2F \rightarrow Li_2F^-$ would create a nascent anion in the equilibrium geometry of the neutral; even in this geometry, Li_2F^- is calculated to be electronically bound, by 0.60 eV vis à vis 0.72 eV in the linear arrangement. Consequently, theory predicts that the successive reduction $Li_2F^+ \rightarrow Li_2F \rightarrow Li_2F^-$ should produce (at least partly) a survivable anion, as substantiated by the $^+CR^-$ spectrum of Fig. 4.

4. Conclusions

Neutralization–reionization mass spectrometry (NRMS) shows that the hypermetalated Li_2F radical resides in a potential energy well, as has been predicted by several theoretical studies. The same is true for the anion Li_2F^-. Dissociation of energetically excited Li_2F^- mainly produces F^- and $LiF^{-\cdot}$, i.e. fragment anions with high electron binding energies. On the other hand, dissociation of collisionally activated Li_2F^+ is found to yield abundant Li^+ and $LiF^{+\cdot}$ which correspond to direct cleavages; however, F^+ becomes the base peak with collision targets of high ionization energy. Our studies are currently being expanded to several other hypermetallic halides, oxides, hydroxides, sulfides, and hydrosulfides to evaluate the stability and reactivity of hypermetalated neutrals (and their ionic forms) as a function of metal ion, heteroatom, and degree of metalation [56].

Acknowledgements

Financial support from the National Science Foundation (CHE-9725003) is gratefully acknowledged. The authors thank Blas A. Cerda and Jianglin Wu for helpful suggestions.

References

[1] P.v.R. Schleyer, E.-U. Würthwein, J.A. Pople, J. Am. Chem. Soc. 104 (1982) 5839.
[2] P.v.R. Schleyer, E.-U. Würthwein, E. Kaufmann, T. Clark, J.A. Pople, J. Am. Chem. Soc. 105 (1983) 5930.
[3] P.v.R. Schleyer, New Horizons in Quantum Chemistry, P.-O. Löwdin, B. Pullman (Eds.), Reidel, Dodrecht, 1983, p. 95.
[4] E.-U. Würthwein, P.v.R. Schleyer, J.A. Pople, J. Am. Chem. Soc. 106 (1984) 6973.
[5] A.I. Boldyrev, P.v.R. Schleyer, J. Am. Chem. Soc. 113 (1991) 9045.
[6] A.I. Boldyrev, I.L. Shamovsky, P.v.R. Schleyer, J. Am. Chem. Soc. 114 (1992) 6469.
[7] G.I. Gutsev, A.I. Boldyrev, Chem. Phys. Lett. 92 (1982) 262.
[8] E. Rehm, A.I. Boldyrev, P.v.R. Schleyer, Inorg. Chem. 31 (1992) 4834.
[9] C. Ochsenfeld, R. Ahlrichs, J. Chem. Phys. 101 (1994) 5977.
[10] (a) S.G. Lias, J.E. Bartmess, J.F. Liebman, J.L. Holmes, R.D. Levin, W.G. Mallard, J. Phys. Chem. Ref. Data 17 (1988) Suppl. No. 1; (b) W.G. Mallard, P.J., Linstrom (Eds.), NIST Chemistry WebBook, NIST Standard Reference Database Number 69, March 1998, National Institute of Standards and Technology, Gaithersburg MD, 20899 (http://webbook.nist.gov).
[11] Y.-W. Hsiao, K.-M. Chang, T.-M. Su, Chem. Phys. 162 (1992) 335.
[12] C.H. Wu, H. Kudo, H.R. Ihle, J. Chem. Phys. 70 (1979) 1815.
[13] K.I. Peterson, P.D. Dao, A.W. Castleman, Jr., J. Chem. Phys. 79 (1983) 777.
[14] P.D. Dao, K.I. Peterson, A.W. Castleman, Jr., J. Chem. Phys. 80 (1984) 563.
[15] A. Goldbach, F. Hensel, K. Rademann, Int. J. Mass Spectrom. Ion Processes 148 (1995) L5.
[16] D.T. Vituccio, R.F.W. Herrmann, O. Golonzka, W.E. Ernst, J. Chem. Phys. 106 (1997) 3865.
[17] L. Bewig, U. Buck, S. Rakowsky, M. Reymann, C. Steinbach, J. Phys. Chem. A 101 (1997) 6538.
[18] T.-C. Kuan, R.-C. Jiang, T.-M. Su, J. Chem. Phys. 92 (1990) 2553.
[19] R.-C. Jiang, T.-M. Su, Chem. Phys. Lett. 181 (1991) 373.
[20] H. Kudo, C.H. Wu, Chem. Express 5 (1980) 633.
[21] H. Kudo, K.F. Zmbov, Chem. Phys. Lett. 187 (1991) 77.
[22] M.M. Kappes, P. Radi, M. Schär, E. Schumacher, Chem. Phys. Lett. 113 (1985) 243.
[23] H. Kudo, M. Hashimoto, K. Yokoyama, C.H. Wu, A.E. Derigo, F.M. Bickelhaupt, P.v.R. Schleyer, J. Phys. Chem. 99 (1995) 6477.
[24] S.L. Wang, K.W.D. Ledingham, R.P. Singhal, J. Phys. Chem. 100 (1996) 11282.
[25] C. Wesdemiotis, F.W. McLafferty, Chem. Rev. 87 (1987) 485.
[26] J.K. Terlouw, H. Schwarz, Angew. Chem., Int. Ed. Engl. 26 (1987) 805.
[27] J.L. Holmes, Mass Spectrom. Rev. 8 (1989) 513.
[28] N. Goldberg, H. Schwarz, Acc. Chem. Res. 27 (1994) 347.
[29] D.V. Zagorevskii, J.L. Holmes, Mass Spectrom. Rev. 13 (1994) 133.
[30] M.J. Polce, Š. Beranová, M.J. Nold, C. Wesdemiotis, J. Mass Spectrom. 31 (1996) 1073.
[31] J. Berkowitz, H.A. Tasman, W.A. Chupka, J. Chem. Phys. 36 (1962) 2170.

[32] S.M. Lin, J.G. Wharton, R. Grice, Mol. Phys. 26 (1973) 317.
[33] C.E. Rechsteiner, R.P. Buck, L. Pedersen, J. Chem. Phys. 65 (1976) 1659.
[34] G.P. Reck, B.P. Mathur, E.W. Rothe, J. Chem. Phys. 66 (1977) 3847.
[35] L. Bengtsson, B. Holmberg, S. Ulvenlund, Inorg. Chem. 29 (1990) 3615.
[36] A.S. Shalabi, J. Mol. Struct. (Theochem) 236 (1991) 371.
[37] A.B. Sannigrahi, P.K. Nandi, P.v.R. Schleyer, Chem. Phys. Lett. 204 (1993) 73.
[38] A. Stintz, J.A. Panitz, J. Vac. Sci. Technol. A 13 (1995) 169.
[39] M.J. Polce, C. Wesdemiotis, Rapid Commun. Mass Spectrom. 10 (1996) 235.
[40] V.G. Solomonik, V.V. Sliznev, T.P. Pogrebnaya, Zh. Strukt. Khim. 29 (1988) 22.
[41] M. Gutowski, J. Simons, J. Chem. Phys. 100 (1994) 1308.
[42] M.J. Polce, M.M. Cordero, C. Wesdemiotis, P.A. Bott, Int. J. Mass Spectrom. Ion Processes 113 (1992) 35.
[43] (a) F.W. McLafferty (Ed.), Tandem Mass Spectrometry, Wiley, New York, 1983; (b) K.L. Busch, G.L. Glish, S.A. McLuckey, Mass Spectrometry/Mass Spectrometry, VCH, New York, 1988.
[44] R.G. Cooks, J.H. Beynon, R.M. Caprioli, G.R. Lester, Metastable Ions, Elsevier, Amsterdam, 1973.
[45] J.L. Holmes, Org. Mass Spectrom. 20 (1985) 169.
[46] A.I. Boldyrev, J. Simons, P.v.R. Schleyer, J. Chem. Phys. 99 (1993) 8793.
[47] C.W. Bauschlicher, Jr., H. Partridge, J. Chem. Phys. 103 (1995) 1788.
[48] P.O. Danis, R. Feng, F.W. McLafferty, Anal. Chem. 58 (1986) 355.
[49] Š. Beranová, C. Wesdemiotis, J. Am. Soc. Mass Spectrom. 5 (1994) 1093.
[50] V.Q. Nguyen, F. Tureček, J. Mass Spectrom. 31 (1996) 843.
[51] F. Tureček, M. Gu, C.E.C.A. Hop, J. Phys. Chem. 99 (1995) 2278.
[52] M. Veljković, O. Neškovič, M. Miletič, K.F. Zmbov, Rapid Commun. Mass Spectrom. 10 (1996) 619.
[53] M.J. Polce, Y. Kim, C. Wesdemiotis, Int. J. Mass Spectrom. Ion Processes 167/168 (1997) 309.
[54] A.B. Raksit, R.F. Porter, Org. Mass Spectrom. 22 (1987) 410.
[55] C. Wesdemiotis, B. Leyh, A. Fura, F.W. McLafferty, J. Am. Chem. Soc. 112 (1990) 8655.
[56] M.J. Polce, S.J. Klippenstein, C. Wesdemiotis, Proceedings of the 46th ASMS Conference on Mass Spectrometry and Allied Topics, Orlando, FL, May 31–June 4, 1998, p. 457.